Biomedical Optics EXPRESS

Spectral analysis of whisking output via optogenetic modulation of vibrissa cortex in rat

R. Pashaie and R. Falk

Electrical Engineering Department, University of Wisconsin-Milwaukee, // 3200 N Cramer St., Milwaukee, WI 53211, USA

pashaie@uwm.edu

https://pantherfile.uwm.edu/pashaie/www/

Abstract: Whisking motor output in awake and freely moving rat is investigated with optogenetic excitation/inhibition of the vibrissae motor cortex (vMCx) layer V. The goal of the study is to establish the direct causal relationship between the cortical activity and the whisking output using optical stimulation, excitatory or inhibitory, with different frequencies. Progression and reduction of the whisking frequency was obtained; however, the whisking frequency did not necessarily followed the entrainment stimulus. Based on our observations, the excitation of the vMCx doubled and inhibition reduced the whisking frequency to half, compared to control, at all stimulus frequencies. This result is an empirical evidence that the cortex exerted control through a central pattern generator structure since complete inhibition was not obtained and the frequency of the response was different from that of the stimulus. We suggest that the use of the optogenetic approach, which enabled us to perform the bidirectional modulation and direct readout from vMCx, has brought valid evidence for the causal connection between cortical activity and whisking motor output.

OCIS codes: 000.1430, 280.1415.

References and links

1. W. I. Welker WI, "Analysis of sniffing of the albino rat," Behaviour **22**(3/4), 223-244, (1964).
2. R. W. Berg and D. Kleinfeld, "Rhythmic whisking by rat: retraction as well as protraction of the vibrissae is under active muscular control," J. Neurophysiol. **89**(1), 104-117, Jan. (2003).
3. G. E. Carvell and D. J. Simons, "Biometric analyses of vibrissal tactile discrimination in the rat," J. Neurosci. **10**(8), 2638-2648, (1990).
4. G. E. Carvell, S. A. Miller, and D. J. Simons, "The relationship of vibrissal motor cortex unit activity to whisking in the awake rat," Somatosens. Mot. Res. **13**(2), 115-127, (1996).
5. R. W. Berg and D. Kleinfeld, "Vibrissa movement elicited by rhythmic electrical microstimulation to motor cortex in the aroused rat mimics exploratory whisking," J. Neurophysiol. **90**(5), 2950-2963, (2003).
6. L. J. Herfst and M. Brecht, "Whisker movements evoked by stimulation of single motor neurons in the facial nucleus of the rat," J. Neurophysiol. **99**, 2821-2832, (2008).
7. K. F. Ahrens and D. Kleinfeld, "Current flow in vibrissa motor cortex can phase-lock with exploratory rhythmic whisking in rat," J. Neurophysiol **92**(3), 1700-1707, (2004).
8. F. Haiss and C. Schwarz, "Spatial segregation of different modes of movement control in the whisker representation of rat primary motor cortex," J. Neurosci. **25**(6), 1579-1587, (2005).
9. R. Izraeli and L. Porter, "Vibrissal motor cortex in the rat: connections with the barrel field," Exp. Brain. Res. **104**(1), 41-54, (1995).

#175994 - $15.00 USD Received 11 Sep 2012; revised 13 Oct 2012; accepted 5 Dec 2012; published 14 Dec 2012

10. D. Kleinfeld, R. W. Berg, and S. M. O'Connor, "Anatomical loops and their electrical dynamics in relation to whisking by rat," Somatosens. Mot. Res. **16**(2), 69-88, (1999).
11. F. Matyas, V. Sreenivasan, F. Marbach, C. Wacongne, B. Barsy, C. Mateo, R. Aronoff, C. Petersen, "Motor control by sensory cortex," Science **330**(6008), 1240-1243, (2010).
12. M. E. Helmet and A. Keller, "Superior colliculus control of vibrissa movements," J. Neurophysiol. **100**(3), 1245-1254, (2008).
13. A. Hattox, Y. Li, and A. Keller, "Serotonin regulates rhythmic whisking," Neuron **39**(2), 343-352, (2003).
14. A. M. Hattox, C. A. Priest, and A. Keller, "Functional circuitry involved in the regulation of whisker movements," J. Comp. Neurol. **442**, 266-276, (2002).
15. E. J. Lang, I. Sugihara, and R. Llins, "Olivocerebellar modulation of motor cortex ability to generate vibrissal movements in rat," J. Physiol. **571**(Pt 1), 101-120, (2006).
16. V. Grinevich, M. Brecht, and P. Osten, "Monosynaptic pathway from rat vibrissa motor cortex to facial motor neurons revealed by lentivirus-based axonal tracing," J. Neurosci. **25**(36), 8250-8258, (2005).
17. W. A. Friedman, L. M. Jones, N. P. Cramer, E. E. Kwegyir-Afful, H. P. Zeigler, and A. Keller, "Anticipatory activity of motor cortex in relation to rhythmic whisking," J. Neurophysiol. **95**(2), 1274-1277, (2006).
18. W. A. Friedman, H. P. Zeigler, and A. Keller, "Vibrissae motor cortex unit activity during whisking," J. Neurophysiol. **107**(2), 551-563, (2012).
19. M. A. Castro-Alamancos, "Vibrissa myoclonus (rhythmic retractions) driven by resonance of excitatory networks in motor cortex," J. Neurophysiol. **96**(4), 1691-1698, (2006).
20. N. P. Cramer and A. Keller, "Cortical control of a whisking central pattern generator," J. Neurophysiol. **96**(1), 209-217, (2006).
21. N. P. Cramer, Y. Li, and A. Keller, "The whisking rhythm generator: a novel mammalian network for the generation of movement," J. Neurophysiol. **97**(3), 2148-258, (2007).
22. A. M. Aravanis, L. P. Wang, F. Zhang, L. A. Meltzer, M. Z. Mogri, M. B. Schneider, and K. Deisseroth, "An optical neural interface: in vivo control of rodent motor cortex with integrated fiberoptic and optogenetic technology," J. Neural Eng. **4**(3), 143-156, (2007).
23. E. S. Boyden, F. Zhang, E. Bamberg, G. Nagel, and K. Deisseroth, "Millisecond-timescale, genetically targeted optical control of neural activity," Nat. Neurosci. **8**(9), 1263-1268, (2005).
24. F. Zhang, V. Gradinaru, A. R. Adamantidis, R. Durand, R. D. Airan, L. de Lecea, and K. Deisseroth, "Optogenetic interrogation of neural circuits: technology for probing mammalian brain structures," Nat. Protoc. **5**(3), 439-456, (2010).
25. I. Diester, M. T. Kaufman, M. Mogri, R. Pashaie, W. Goo, O. Yizhar, C. Ramakrishnan, K. Deisseroth, and K. V. Shenoy, "An optogenetic toolbox designed for primates," Nat. Neurosci. **14**(3), 387-397, (2011).
26. R. Pashaie and R. Falk, "Single optical fiber probe for fluorescence detection and optogenetic stimulation," IEEE Trans. Biomed. Eng. (to be published).
27. K. Frimpong and S. A. Spector, "Cotransduction of nondividing cells using lentiviral vectors," Gene. Ther. **7**(18), 1562-1569, (2000).
28. O. G. Ayling, T. C. Harrison, J. D. Boyd, A. Goroshkov, and T. H. Murphy, "Automated light-based mapping of motor cortex by photoactivation of channelrhodopsin-2 transgenic mice," Nat. Methods, **6**(3), 219-224, (2009).
29. M. A. Castro-Alamancos, "Neocortical synchronized oscillations induced by thalamic disinhibition in vivo," J. Neurosci. **19**(18), RC27 1-7, (1999).
30. M. A. Castro-Alamancos, "Origin of synchronized oscillations induced by neocortical disinhibition in vivo," J. Neurosci. **20**(24), 9195-9206, (2000).
31. A. B. Ali, J. Rossier, J. F. Staiger, and E. Audinat, "Kainate receptors regulate unitary IPSCs elicited in pyramidal cells by fast-spiking interneurons in the neocortex," J. Neurosci. **21**(9), 2992-2999, (2001).
32. M. Y. Min, Z. Melyan, and D. M. Kullmann, "Synaptically released glutamate reduces gamma-aminobutyric acid (GABA)ergic inhibition in the hippocampus via kainate receptors," Proc. Natl. Acad. Sci. USA **96**, 9932-9937, (1999).
33. M. Brecht, V. Grinevich, T. E. Jin, T. Margrie, and P. Osten, "Cellular mechanisms of motor control in the vibrissal system," Pflugers. Arch. **453**(3), 269-281, (2006).
34. P. Gao, R. Bermejo, and H. P. Zeigler, "Whisker deafferentation and rodent whisking patterns: behavioral evidence for a central pattern generator," J. Neurosci. **21**(14), 5374-5380, (2001).
35. P. Gao, A. M. Hattox, L. M. Jones, A. Keller, and H. P. Zeigler, "Whisker motor cortex ablation and whisker movement patterns," Somatosens. Mot. Res. **20**(3-4), 191-198, (2003).
36. D. L. Sodickson and B. P. Bean, "GABAB receptor-activated inwardly rectifying potassium current in dissociated hippocampal CA3 neurons," J. Neurosci. **16**(20), 6374-6385, (1996).
37. S. Kleinlogel, U. Terpitz, B. Legrum, D. Gkbuget, E. Boyden, C. Bamann, P. Wood, and E. Bamberg, "A gene-fusion strategy for stoichiometric and co-localized expression of light-gated membrane proteins," Nat. Methods **8**(12), 1083-1088, (2011).

#175994 - $15.00 USD Received 11 Sep 2012; revised 13 Oct 2012; accepted 5 Dec 2012; published 14 Dec 2012

1. Introduction

The study of motor control output in general and of specific systems like whisking in particular, has been a permanent case for investigation in neurophysiology. Fast rhythmic vibrissae movements are used by rodents to explore the environment [1]. The so called active exploratory whisking is a combination of protraction followed by retraction movement within an anteroposterior horizontal plane, in air and over objects at frequencies of 4 to 15Hz recorded by electrodes [2, 3, 4]. Rhythmic movements similar to exploratory whisking and small vibrissa retractions can be triggered by electric low intensity stimulation of the medial areas of the motor cortex [5, 6, 8]. This area is considered as the vibrissa motor cortex (vMCx) which affects whisking via producing reciprocal projections with the barrel cortex [9, 10, 11] and premotoneuron networks that forms a central pattern generator (CPG) distributed throughout the mid- [12] and hindbrain [13, 14, 15]. In addition, vMCx projects directly to facial motorneurons providing a route to control vibrissae movements [16], the coordinator [6, 7, 17, 18], and also a part of the CPG [19, 20, 21].

More profound understanding in the field could be generated using new experimental paradigms in conjunction with recent methodologies. Such a recent method is optogenetics [22, 23, 24] which has opened the possibility for selective targeting of neuronal subpopulation to stimulate or inhibit neural activities by exposing the cells to appropriate wavelengths. For this purpose, genetically targeted neurons express opsins, such as channelrhodopsin 2 (ChR2) and halorhodopsin (eNpHR) fused in frame with enhanced yellow fluorescent protein (EYFP), under the control of a neuron type specific promoter, e.g., Ca^{2+}/calmodulin dependent proteinkinase II α (CaMKIIα) which mostly targets the excitatory pyramidal neurons. Expression of ChR2 enables the neuron to be depolarized by blue light exposure at 473nm and eNpHR to hyperpolarize by yellow light with peak sensitivity at 593nm. Using the optogenetic toolbox, by co-expression of both opsins, one can interrogate the vMCx using this novel method which is different from the electrical intracortical microstimulation (ICMS) which known to be the classical approach in neurophysiology. Taking advantage of an integrated dual laser single optical fiber device [26, 25] that is developed in our lab and can be used for both excitation and detection of fluorescence simultaneously, we developed an optogenetic paradigm for the study of the modulation of whisking motor output through the vMCx in the awake, unconditioned freely moving rat. We hypothesize that after co-expression of ChR2 and eNpHR under control of CaMKIIα promoter in the pyramidal neurons of the layer V in the vMCx of the rat [27], we should be able to manipulate the whisking behavior and retrieve characteristic parameters of the process.

2. Materials and Methods

Experiments were carried out in accordance with the National Institutes of Health (NIH) guidelines for the care and use of laboratory animals. Experimental protocols were approved by the IACUC of the University of Wisconsin-Milwaukee.

This study reports the experiments performed on six Sprague Dawley female rats, all being surgically instrumented for implantation of optical neural interface. Of these, four were stereotactically injected with lentivirus mixture for co-expression of ChR2 and eNpHR and two with phosphate buffered saline (PBS) as controls. The animals have been only gentled, not trained or conditioned for any task. Experiments started after 30 days allowing the expression level for the ChR2 and eNpHR to attain the acceptable values for experiments.

#175994 - $15.00 USD Received 11 Sep 2012; revised 13 Oct 2012; accepted 5 Dec 2012; published 14 Dec 2012

2.1. *Lentivirus production and titering:*

The expression plasmids pLenti-CaMKIIα-ChR2(H134R)-EYFP-WPRE (courtesy of Dr. Karl Deisseroth, Stanford University) and pLenti-CaMKIIα-eNpHR-EYFP-WPRE (Addgene, Cambridge, MA) were each co-transfected with the plasmids pCMVR8.74 and pCMV-VSV-G (Addgene, Cambridge, MA) via calciumphosphate (Clontech, Mountain View, CA) of HEK 293FT cells (Invitrogen, Grand Island, NY) high titer lentivirus ($> 10^6$ i.u./ml) was then packaged. Then, 24*h* post-transfection, HEK 293FT cells were switched to serum-free medium Optimem (Invitrogen, Grand Island, NY); the supernatant was collected 24*h* later and concentrated 1000*x* by ultrafiltration (Pall Co, Ann Arbor, MI). The resulting lentiviral concentrate titering was performed in HEK293 cells that were grown in 24-well plates and inoculated with 5-fold serial dilutions. After 4 days, cultures were resuspended in PBS and counted for EYFP expression in hemacytometer (Hausser Sci, Horsham, PA). The titer of the virus was determined by: [(% of infected cells) $\times$ (total number of cells in well) $\times$ (dilution factor)]/ (volume of inoculum added to cells) = infectious units (i.u.)/ml. The titer of concentrated lentivirus for *in-vivo* injection was 10^9 i.u. /ml. An equal titer mixture 1 : 1 of concentrated lentiviruses was used for the co-expression of ChR2-EYFP and eNpHR-EYFP.

2.2. *Implantation of optical neural interface and stereotaxic injection into the brain:*

Female rats $250g - 350g$ were the subjects of these experiments. Concentrated lentivirus solution was stereotactically injected into the rat vibrissae motor cortex (anterior-posterior = 1.5*mm* from bregma; lateral = 1.5*mm*; ventral = 1.5*mm*) corresponding to layer V.

All surgeries were performed under aseptic conditions. The animals were anesthetized with isoflurane $1.5 - 2\%$ isoflurane in 95% oxygen. The head was shaved, cleaned with 70% ethanol and betadine and then placed in a digital lab standard stereotaxic apparatus (Stoelting Co, Wood Dale, IL). Ophthalmic ointment was applied to prevent eye drying. A midline scalp incision was made and then a small craniotomy was performed using a drill mounted on the stereotaxic apparatus (Foredom Electric Co, Bethel, CT). A cannula guide C313G (PlasticsOne, Roanoke, VA) was then inserted through the craniotomy to a depth of $1mm$ ($800\mu m$ across frontal bone and $200\mu m$ into the brain). Three plastic skull screws $00 - 96x3/32$ (PlasticsOne, Roanoke, VA) were placed in the skull surrounding the cannula guide pedestal, and cranioplastic cement (Pearson Dental, Sylmar, CA) was used to anchor the cannula guide system to the skull screws. The virus was delivered using a $10\mu l$ syringe and a thin 35 gauge blunt metal needle passing through the cannula guide; the injection volume and flow rate ($1\mu l$ at $0.1\mu l$/min) was controlled with an injection pump from (World Precision Instruments, Sarasota, FL). After injection the needle was left in place for 10 additional minutes for diffusion of the lentivirus, and then slowly withdrawn and a dummy cannula C313G (PlasticsOne, Roanoke, VA) was inserted to keep the cannula guide open. The free edge of the scalp was brought to the base of the cranioplastic cement using sutures $3 - 0$ silk (Ethicon, Somerville, NJ) and tissue adhesive Vetbond (3M, St. Paul, MN). The animal was kept on a heating pad until it recovered from anesthesia. Lidocaine 0.5% gel was applied on the scalp following the surgical procedure to minimize discomfort. The cannula guide also functions as the optical fiber guide. In order to be positioned at the desired depth in the brain, the tip of the optical fiber has a glued stopper so that when inserted into the guide it extends exactly 1.5*mm* from the base of the guide and 0.5*mm* out of the guide. Before gluing the stopper, the fiber is passed through a hole in a plastic dust cap, which glides freely on the fiber and screwing it to the pedestal of the fiber guide, secures the optical interface to the skull of the rat stabilizing the tip of the optical fiber at 1.5*mm* depth measured from the surface of the skull. The tip of the fiber is positioned at the $700\mu m$ depth within the motor cortex which corresponds to layer V.

#175994 - $15.00 USD Received 11 Sep 2012; revised 13 Oct 2012; accepted 5 Dec 2012; published 14 Dec 2012

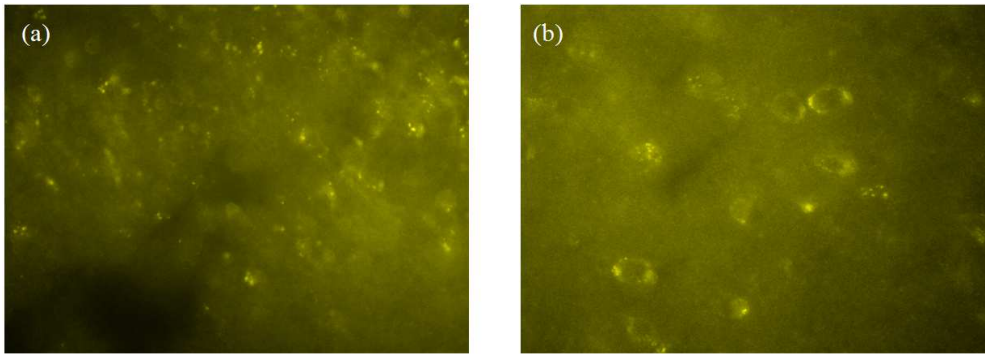

Fig. 1. Fluorescence images that displays the EYFP expression in a fresh coronal slice at the site of lentivirus injection. (a) 20X magnification. (b) 40X magnification.

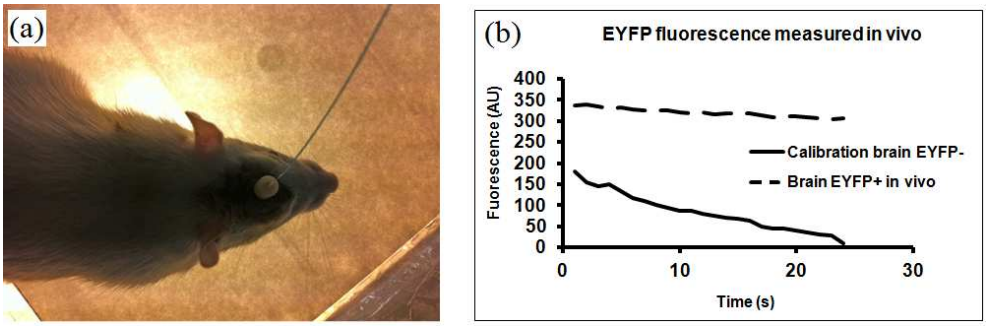

Fig. 2. (a) Rat with optical fiber implant inside the arena, (b) Fluorescence measurement *in-vivo*. The fluorescence signal presented in arbitrary units, was measured for 25*s* in an EYFP negative brain for calibration and then it was measured for the same period in the brain of an EYFP positive rat at the injection site in vibrissa motor cortex. Notice the exponential photo bleaching in the calibration brain comparative to the steady signal in the EYFP positive brain.

2.3. Stimulation with light of pyramidal neurons in layer V of vibrissa motor cortex:

Stimulation of ChR2+/eNpHR+ neurons was accomplished using a multimode optical fiber ($NA = 0.22$) with a $200\mu m$ silica core FG200UGG (Thorlabs, Newton, NJ) coupled to a $473nm$ blue laser LRS-0473 Series of Diode-Pumped Solid-State (DPSS) and a $593nm$ yellow laser LRS-0594 DPSS (Laserglow Technologies, Toronto, ON, Canada). The measured light intensity emanating from the tip of the fiber was $160mW/mm^2$ [28]. The distal end of the fiber was polished and the jacket was stripped; the fiber was inserted into the fiber guide and advanced until flush with the fiber guide end. The animal was then allowed to habituate to the setup.

2.4. Whisker movement recording, frequency and mean angular deflection measurement:

Animals were awake and freely moving. Whiskers contralateral to the fiber guide implantation were video recorded from above the head while the rat is placed inside the arena. The arena in this experiment is a plastic uncovered rat cage illuminated from the bottom through a thin white paper sheet which helps to gain diffuse background lighting. This setup allows to see clearly the vibrissae particularly in contrast inverted images produced by ImageJ (NIH, Bethesda, MA). We used a digital camera, Power Shot SX230 HS (Canon, Lake Success, NY), with 30 frames

#175994 - $15.00 USD Received 11 Sep 2012; revised 13 Oct 2012; accepted 5 Dec 2012; published 14 Dec 2012

per second temporal resolution and spatial resolution of $100 - 200\mu m$, to monitor the motion of the vibrissae along the anterior-posterior axis only. ImageJ was used to track movement in the video. For this purpose, one linear vector of pixels in the image in the vicinity of the chosen whisker and parallel to its direction was selected in the captured frames and the value of the associated pixels were extracted for all frames along the time-laps. This vector of pixels function as twitching detectors. Whenever the whisker moves the intensity of these pixels drops which indicates a whisker twitching event. This algorithm can be applied for the case when animal does not move in the arena during the period we record the signal. In case animal moves or the head of the animal moves that data should be discarded. Also using ImageJ angle tool, we measured whiskers mean deflection angle for different frequencies of light stimulus for each of the two wavelengths: 473*nm* and 593*nm*. Experiments were initiated once the animal stopped exploring the experimental arena and did not move the head. During an experimental sweep, 20*s* of pre-stimulus data, 20*s* of intra-stimulus data (20*s* pulse of blue or yellow light) and 20*s* of post-stimulus data were recorded. We noticed that 20*s* period is relatively good timing over which we can frequently find the animal staying with almost no movement in a part of arena. Therefore, 20*s* period was reasonable to record the data when animal was free to move but not moving.

2.5. Slice preparation and epi-fluorescence imaging:

For preparation of brain slices, one rat was sacrificed 9 days after viral injection. Acute coronal brain slices (100μm) were prepared in ice-cold cutting solution (64 mM NaCl, 25 mM NaHCO3, 10 mM Glucose, 120 mM Sucrose, 2.5 mM KCl, 1.25 mM NaH2PO4, 0.5 mM CaCl2, 7 mM MgCl2) using a vibratome (Lancer Series 1000; Vibratome Company, St. Louis, MO). The slices were then fixed for one hour in 4% paraformaldehyde, washed with PBS and mounted on microscope slides. Images of EYFP fluorescent neurons were recorded with a cooled CCD camera Exi Aqua (Qimaging, Surrey, BC, Canada) on an upright BX51WI Olympus microscope (Olympus America Inc., Center Valley, PA) and a EYFP filter set: excitation filter BP490-500HQ, dichroic DM505HQ (Olympus America Inc., Center Valley, PA).

2.6. In-vivo measurement of EYFP fluorescence as a measure of the level of opsin expression:

Because the standard histological methods require sacrificing the animal, thus terminating experiments, it would be desirable to determine expression levels *in-vivo* while experiments are ongoing.

This would allow monitoring expression levels over the weeks following the injections and determining the ideal time point for starting the work with the respective animal subject. The fluorescence detection device achieves this goal, which for optimal versatility and minimal tissue damage employing a single fiber optic cable both to deliver source light as well as to detect the EYFP emitted fluorescent light. In this design, the same fiber can be used to deliver light for neural modulation (when used for optogenetic experiments) as well as to deliver light for fluorescence excitation (when used for *in-vivo* fluorescence measurements). The fiber delivers excitation light pulses to the region of interest, and guides a sample of the corresponding emission signal back to a sensitive low-noise detector.

Parallel to this first photodetector, a second detector is employed to eliminate the effect of input light fluctuations, imperfection of the optical filters, self-fluorescence at the tip of the fiber, and random back-reflection of the excitation or stimulation light within tissue. A set of optical fiber splitters are used to combine the input light that is generated by numerous light sources and to distribute the emission signal in the system [26, 25]. A combination of patterned pulses and a software based time-lens filter is used to further improve the signal to noise ratio. Compared to traditional dichroic based setups, the new system is smaller in size and mobile,

#175994 - $15.00 USD Received 11 Sep 2012; revised 13 Oct 2012; accepted 5 Dec 2012; published 14 Dec 2012

robust, and requires minimal alignment. The device has a FC/PC connector which is used to attach an optical fiber that we insert into the vMVx of the animal under test. Fluorescence measurements were performed *in-vivo* after calibration of the device. To measure the EYFP expression level we used 473*nm* light for excitation while emission optical filter with center wavelength 545*nm* in front of the sensitive photodetector.

3. Results

3.1. Co-expression of ChR2 and eNpHR by dual lentiviral infection in vivo:

Dual lentiviral infection of the pyramidal neurons in layer V of the right vMCx in rat was achieved by stereotaxic injection of $1\mu L$ of equal titer lentiviral mixture of p-Lenti-CaMKIIα-ChR2-EYFP and p-Lenti-CaMKIIα-eNpHR-EYFP. The control rat was injected with phosphate buffered saline (PBS). The preference for expression of ChR2 and eNpHR from separate transgenes and not taking advantage of a stoichiometric and co-localized gene-fusion strategy is justified by a more natural and even distribution of the constructs which are already a form of fused structures, carrying EYFP [37]. A morphologic control was necessary in order to make sure we obtained the expression *in-vivo* at the desired stereotaxic coordinates. After nine days, one lentiviral injected rat was sacrificed, the brain was extracted and fresh coronal slices $100\mu m$ were prepared from the region of interest and the level of expression was checked by fluorescence microscopy (Figure 1). Once the success of gene delivery and protein expression was confirmed in the test rat, in our next step, we used our single optical fiber fluorescence probe to evaluate the level of EYFP expression *in-vivo* 30 days after injection (Figure 2). Details of fluorescence detection is explain in reference [26].

3.2. Continuous versus chirped pulse stimulation:

Initial test of excitation or inhibition of neurons in layer V of vMCx was done either with continuous stimulus for 20*s* or 20 chirped pulses (linear chirp pulse where frequency is swept from 0*Hz* to 100*Hz* over period of 1*s* for each pulse 1*s* [26]). Blue light 473*nm*, both continuous and chirped stimulus, enhanced the whisking activity significantly compared to pre and post-stimulus (events/s: intra-stimulus continuous 1.6 ± 0.19; pre-stimulus 0.74 ± 0.02; post-stimulus 0.79 ± 0.09, two-tailed t tests $p < 0.02$ (Figure 3a) and intra-stimulus chirped 1.92 ± 0.23 ; pres-stimulus 0.7 ± 0.07; post-stimulus 0.87 ± 0.05, two-tailed t tests $p < 0.02$ (Figure 3b)) and also compared to control (two-tailed t tests: $p < 0.05$ for continuous and $p < 0.02$ for chirped stimulus, respectively (Figure 3ab). The chirped stimulus seemed to be slightly more efficient compared to continuous stimulus ($p = 0.18$). Inhibition of whisking activity with yellow light 593*nm* was achieved with both continuous and chirped stimulus and the change is significant compared to pre and post-stimulus (events/s: intra-stimulus continuous 0.3 ± 0.08; pre-stimulus 0.8 ± 0.07; post-stimulus 0.7 ± 0.08, two-tailed t tests $p < 0.02$ (Figure 3c) and intra-stimulus chirped 0.30 ± 0.08 ; pre-stimulus 0.76 ± 0.07; post-stimulus 0.7 ± 0.08, two-tailed t tests $p < 0.02$ (Figure 3d)) and also compared to control (two-tailed t tests: $p < 0.05$ for continuous and chirped stimulus, respectively (Figure 3c, d)). Similarly, inhibitory chirped pulses are slightly more efficient compared to continuous yellow light exposure ($p = 0.38$).

These results confirmed that modulation of the whisking behavior in the rat could be done reliably for both excitation and inhibition and that the pulsed stimulus had an apparent greater efficiency. This was also the functional test to prove that the expression of ChR2 and eNpHR was obtained in the pyramidal neurons of layer V in the vMCx.

#175994 - $15.00 USD Received 11 Sep 2012; revised 13 Oct 2012; accepted 5 Dec 2012; published 14 Dec 2012

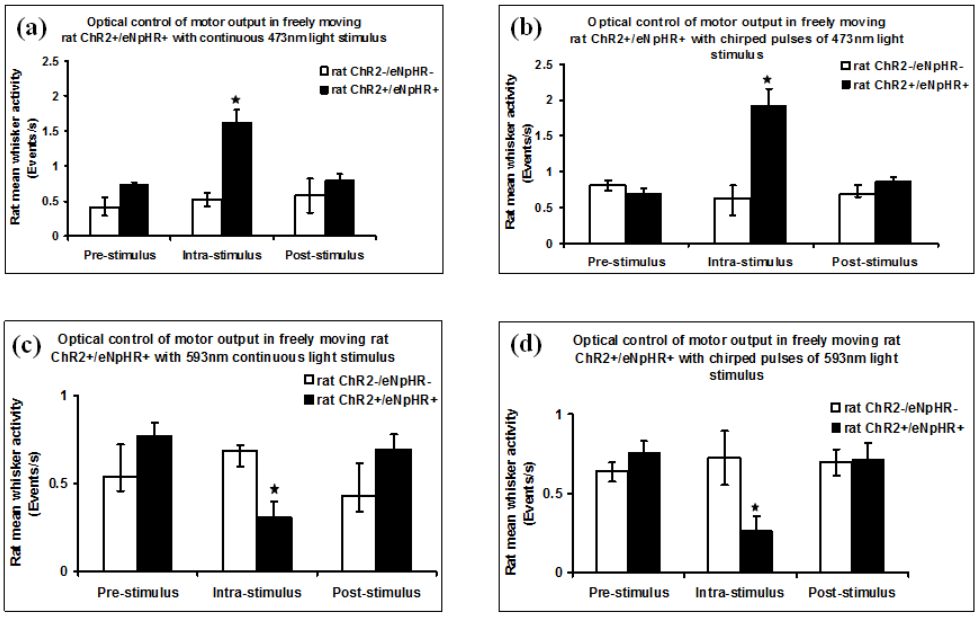

Fig. 3. Mean rate of whisker twitching pre-stimulus, intra-stimulus and post-stimulus. The mean number of whisker twitching events dramatically increases in the ChR2+/eNpHR+ (lentivirus injected) rats under continuous and chirped blue light ($473nm$) stimulation for $20s$ compared to ChR2-/eNpHR- rats (vehicle injected) (a), (b), $*p < 0.05$, and significantly reduced when stimulated with continuous or chirped yellow laser pulses ($593nm$) for $20s$ (c), (d), $*p < 0.05$.

3.3. Various constant frequency pulsed stimulation:

We decided to test different constant frequency stimuli of: 5, 10, 15, 20, 25, 50, 70 and $90Hz$ for both excitation ($473nm$) and inhibition ($593nm$) light exposure, to evaluate the degree of entrainment of whisking in comparison to the stimulus frequency. The stimulus trains of $20s$ for both wavelengths were formed by square pulses of $10ms$ for the frequencies from $5Hz$ - $25Hz$, $5ms$ for frequencies of 50 and $70Hz$ and $2ms$ for $90Hz$. The results show that the excitation did not entrain the whisking activity to the stimulus frequency but attained a maximum of approximately $3Hz$. Also, we could not achieve the complete inhibition. Based on our observation, under yellow light stimulation the rate of twitching reduced but remained persistently at a value around $0.5Hz$. The values of whisking activity in the control rat were between $1Hz$ to $2Hz$ under exposure with both wavelengths (Figure 4). The $5Hz$ light pulses produce neither stimulation at $473nm$ nor inhibition at $593nm$ compared to pre-stimulus or post-stimulus and also the control rat data (two-tailed t tests: pre ($473nm$) $p = 0.20$, post ($473nm$) $p = 0.10$, control ($473nm$) $p = 0.7$ and pre ($593nm$) $p = 0.57$, post ($593nm$) $p = 0.82$, control ($593nm$) $p = 0.37$, (Figure 4a, b)). Starting with the frequency of $10Hz$ and up to $90Hz$ the stimulus trains over the period of $20s$ triggered significant stimulation of whisking activity at $473nm$ or inhibition at $593nm$ (two-tailed t tests $p < 0.05$ for all comparisons with: pre-stimulus, post-stimulus and control data (Figure 4c to 4p)). This clear non-entraining response of whisking activity when exciting the vMCx with $473nm$ light centered in the band of $1Hz$ - $4Hz$ and the reduction without cancelation when inhibited with $593nm$ light in the frequency band of $0Hz$ - $1Hz$ led us to analyze the spectral properties of the whisking signal.

We performed a moving window analysis with a Short Time Fourier Transform (STFT) of

#175994 - $15.00 USD Received 11 Sep 2012; revised 13 Oct 2012; accepted 5 Dec 2012; published 14 Dec 2012

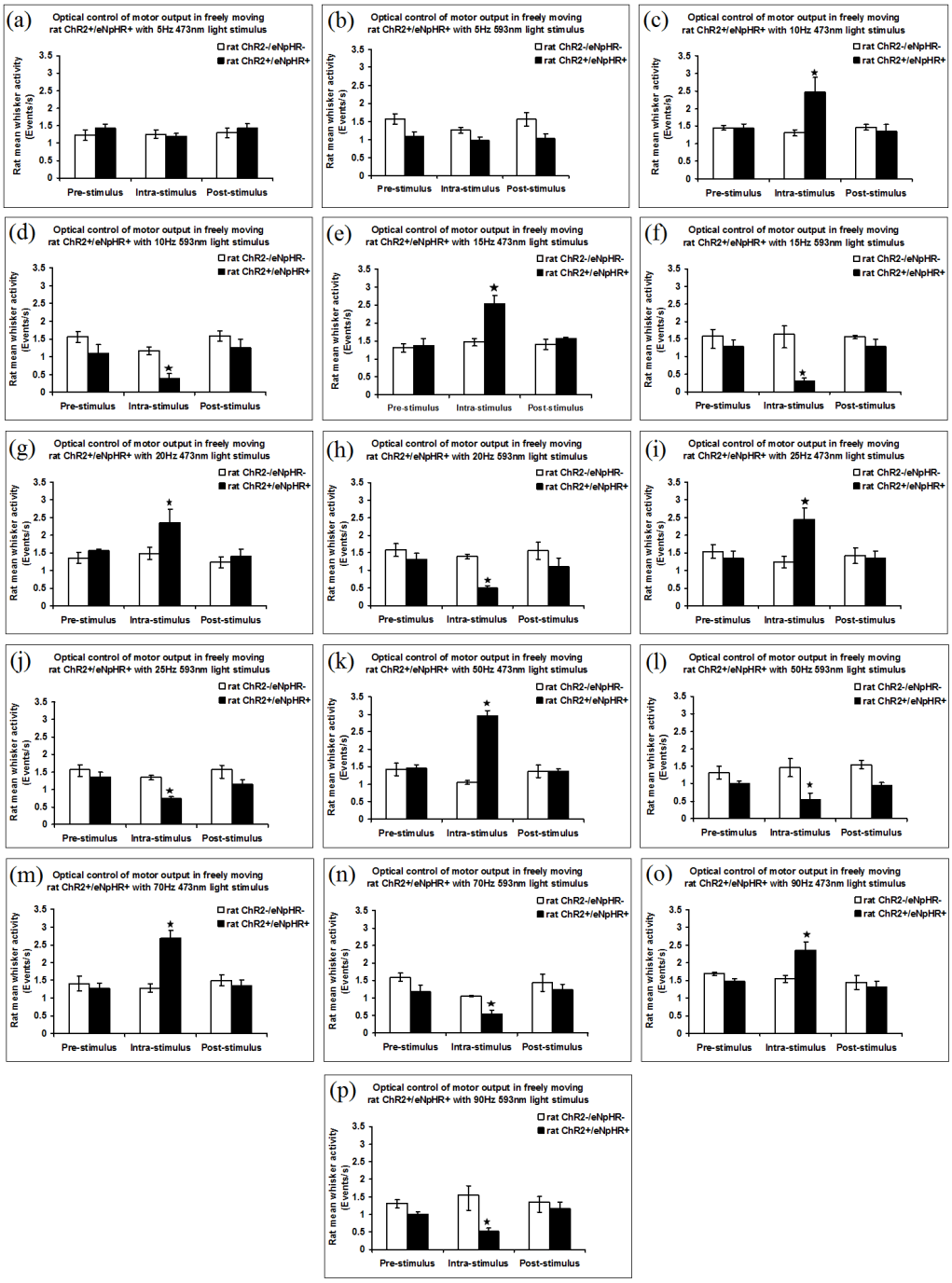

Fig. 4. Optical control of motor output in rat. The mean number of whisker twitching events was significantly greater in the ChR2+/eNpHR+ rats (lentivirus injected) compared to the ChR2-/eNpHR- rats (PBS injected) stimulated with 20*s* train of 10*ms* (10*Hz*-25*Hz*), 5*ms* (50*Hz*-70*Hz*) and 2*ms* (90*Hz*) pulses of 473*nm* light (a), (c), (e), (g), (i), (k), (m), (o), $*p < 0.05$, and significantly smaller when stimulated with 20*s* train of 10*ms* (10*Hz*-25*Hz*), 5*ms* (50*Hz*-70*Hz*) and 2*ms* (90*Hz*) pulses of 593*nm* light for 20*s* (b), (d), (f), (h), (j), (l), (n), (p) $*p < 0.05$.

#175994 - $15.00 USD Received 11 Sep 2012; revised 13 Oct 2012; accepted 5 Dec 2012; published 14 Dec 2012

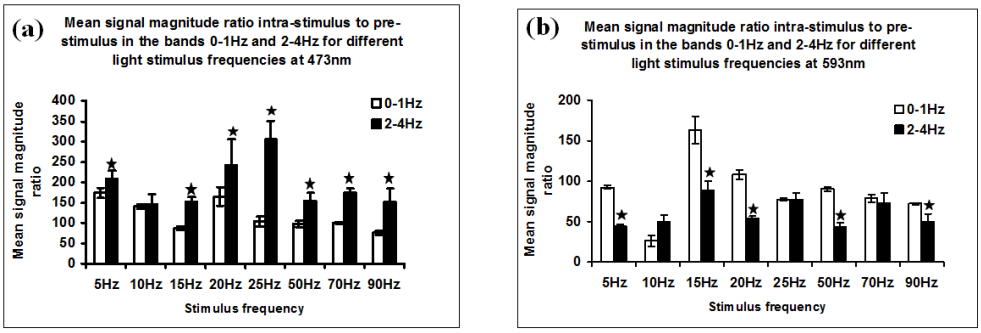

Fig. 5. Changes in frequency characteristics of whisking activity produced by optical stimulation. In this analysis, we looked at two frequency bands of whicker twitching data which are $0Hz$ - $1Hz$ and $2Hz$ - $4Hz$, (a) Under blue light ($473nm$) illumination, the activity recorded in both frequency bands more or less increased for stimulation frequencies of $5Hz$ - $20Hz$ but only the activity in the second band, $2Hz$ - $4Hz$, increased for $25Hz$ - $90Hz$ stimulation pulses. At all frequencies the magnitude of the signal in the $2Hz$ - $4Hz$ band was more than the $0Hz$ - $1Hz$ band. (b) Activity in $2Hz$ - $4Hz$ frequency band reduced at all stimulus frequencies under $573nm$ exposure and the magnitude of the signal was, in general, larger in the $0Hz$ - $1Hz$ band. Except stimulus frequencies of $15Hz$ and $20Hz$, the activity in the $0Hz$ - $1Hz$ band also reduced under $573nm$ illumination.

the whisking signal and focused on the bands centered on the $0.5Hz$ and $3.0Hz$. The data shows that stimulation with $473nm$ (excitation) increases the power of the signal in both bands $0Hz$ - $1Hz$ and $2Hz$ - $4Hz$ above a baseline at all stimulation frequencies which was more noticeable in the frequency range of $2Hz$ - $4Hz$ compared to $0Hz$ - $1Hz$ (two-tailed t tests $p < 0.05$ (Figure 5a)). The stimulation with $593nm$ (inhibition) decreases the power of the signal in the frequency range of $2Hz$ - $4Hz$ under a baseline at all stimulation frequencies. The scenario was the same for the $0Hz$ - $1Hz$ band with the exception for the stimulation frequencies of $15Hz$ and $20Hz$. The power in the band $0Hz$ - $1Hz$ compared to the band $2Hz$ - $4Hz$ increased significantly at all frequencies (two-tailed t tests $p < 0.05$ (Figure 5b)). The parameters which we retrieved with the optogentic paradigm are important since they characterize the vibrissa motor cortex and its relation to the hypothetical CPG.

3.4. Amplitude of whisker deflection at various frequencies of pulsed optical stimulation:

To develop a more complete picture of the vMCx motor output, we also examined the amplitude of the whisker movement. The video recordings were analyzed frame-by-frame and the maximum angular deflection of the whiskers were measured using the angle tool of ImageJ software. Based on our observations, the optical stimulation of vMCx by $473nm$ laser in the frequency range of $5Hz$ to $20Hz$ caused relatively linear increase in the deflection angle of the contralateral whiskers (paired one-tailed t tests $*p < 0.05$ (Figure 6a)). The maximum was attained at $25Hz$ followed by a nonlinear decrease from $25Hz$ to $90Hz$ which still remains significantly larger than the pre-stimulus control values (paired one-tailed t tests $*p < 0.05$ (Figure 6a)). When stimulation was performed with the $593nm$ wavelength, the angular deflection of the whiskers reduced considerably compared to the pre-stimulus control values at all the frequencies (paired one-tailed t tests $*p < 0.05$ (Figure 6b)). We noticed a trend of almost linear decrease from $5Hz$ to $25Hz$ in the angular amplitude of whisker movements with plateau at $50Hz$ and a slight raise at $70Hz$ and $90Hz$. The angular amplitude of the whisker movement showed stronger dependence on the frequency of entrainment compared to the frequency of the

#175994 - $15.00 USD Received 11 Sep 2012; revised 13 Oct 2012; accepted 5 Dec 2012; published 14 Dec 2012

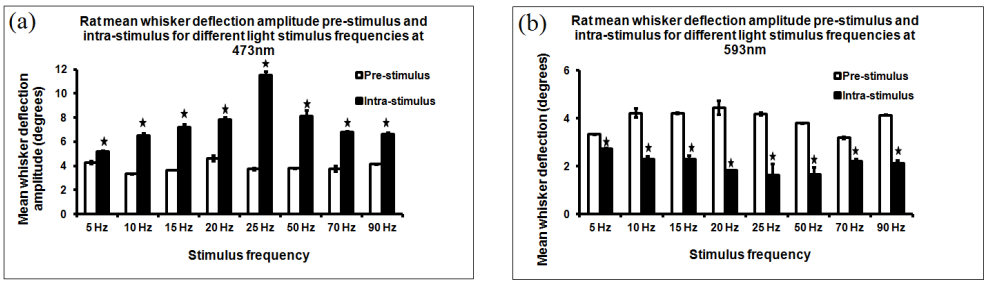

Fig. 6. Mean whisker deflection amplitude at various frequencies of optical stimulation. (a) Mean whisker deflection amplitude significantly increased at all stimulation frequencies under blue light exposure, $*p < 0.05$. (b) Mean whisker deflection amplitude significantly decreased at all stimulation frequencies under yellow light exposure, $*p < 0.05$.

whisker movement. Interestingly, for the domain of natural frequencies of whisking behavior ($5Hz$ - $20Hz$) we noticed a relatively linear dependence of the amplitude of whisking, for both excitation at $473nm$ and inhibition at $593nm$, which points toward the conclusion that vMCx, in this frequency range, controls such aspect of the whisker movement in a more precise manner.

4. Conclusion

Whisking behavior in rat is one of the most investigated processes that covers from the anatomical substrate to cortical activities. Understanding how the motor cortex imposes control over a simply patterned motor activity, such as whisker twitching, helps us to develop models for more complex movements like limb activities. The voluntary control of a rat on the whisking behavior can be correctly understood in awake, unconditioned, freely moving animal which is instrumented with an appropriate neural interface that allows researchers to modulate the activity of pyramidal neurons in layer V of the vMCx. While the classical ICMS assures precise control of the stimulus delivery, it excites all the neuronal populations in the vicinity of the electrode with no specificity. Although most of the knowledge we presently have in neurophysiology is based on the electric stimulation, with the advent of optogenetic tools we can characterize and investigate the motor cortex using light to specifically target the neuronal population of interest.

As we hypothesized, by optogenetic targeting of pyramidal neurons in layer V of the vMCx in a rat and co-expression of ChR2 and eNpHR, we can study the whisking behavior and retrieve parameters which characterize the dynamics of the motor cortex and the putative CPG through which this activity is controlled. In our attempt to drive the vMCx with blue laser pulses of different frequencies, changing from $5Hz$ to $90Hz$, we obtained a maximum vibrissae response happening at $\sim 3Hz$ which it is quite different from the stimulation frequencies. This is a piece of evidence that the vibrissa motor cortex acts by modulating a CPG. Nonetheless, the CPG in cause might be the vMCx itself. This is possible since in our paradigm by stimulating only the pyramidal neurons of layer V, and not the inhibitory interneurons as it happens in ICMS, we triggered neocortical synchronized oscillations induced by thalamic disinhibition [29, 30, 31, 32, 36]. The resultant frequency is $3Hz$ [29, 30] which is apparently generated in the vMCx itself. The second piece of evidence is the fact that the stimulation of the motor cortex by $593nm$ light stimulus did not completely suppress the whisking activities which continued at a frequency $< 1Hz$ ($\sim 0.5Hz$).

We obtained the maximum frequency of $\sim 3Hz$ for vibrissae at any stimulation frequency which was also using the ICMS [10] or single neuron stimulation in vMCx layer V [6, 7, 33]. The whisking frequency of $< 1Hz$ ($\sim 0.5Hz$) was observed when the vibrissa motor cortex was

#175994 - $15.00 USD Received 11 Sep 2012; revised 13 Oct 2012; accepted 5 Dec 2012; published 14 Dec 2012

inhibited by 593*nm* light pulses which functionally mimics the ablation of the motor cortex where the whisking frequency drops under 2*Hz* [34, 35].

Here we presented experimental results where the whisking motor output was optically modulated through the vMCx and we presented some evidences that this activity is controlled by a CPG [20]. We used optogenetic toolbox to extract some fundamental parameters of whisking behavior in awake, unconditioned, freely moving rats.

5. Acknowledgement

The author would like to thank the University of Wisconsin-Milwaukee Research Growth Initiative (RGI) program for providing the financial support for this research under grant numbers 101X172, and 101X213.

#175994 - $15.00 USD Received 11 Sep 2012; revised 13 Oct 2012; accepted 5 Dec 2012; published 14 Dec 2012